SIMOMM: An Integrated Molecular Orbital/Molecular Mechanics Optimization Scheme for Surfaces

James R. Shoemaker[†] and Larry W. Burggraf*

Air Force Institute of Technology, Wright-Patterson AFB, Ohio 45433

Mark S. Gordon*

Department of Chemistry, Iowa State University, Ames, Iowa 50011

Received: June 12, 1998; In Final Form: November 20, 1998

Reactions on surfaces are often modeled using molecular clusters which are too small to accurately represent the mechanical environment of bulk materials. The small size of these clusters is driven by the large cost of ab initio quantum mechanical (QM) computational methods needed to accurately model chemical reactions. Hybrid computational approaches that interface quantum mechanics with molecular mechanics (MM) methods, commonly referred to as QM/MM methods, are becoming increasingly popular for treating large systems, but these hybrid methods have not been applied to surface models. This paper presents a QM/MM optimization scheme for modeling surfaces that is based on the IMOMM approach of Maseras and Morokuma. The modified method, (S)urface IMOMM, and its applications to surface chemistry are discussed.

I. Introduction

The term "surface" chemistry is somewhat misleading, because reactions on surfaces involve more than the uppermost layer of atoms. Subsurface atoms move in response to displacements of surface atoms. For example, X-ray diffraction studies of dimer formation on the silicon(001) surface find that atoms are displaced from lattice positions as deep as eight layers below the surface. These subsurface displacements result from surface atom displacements that occurred during dimer formation.[1] In turn, surface atom displacements are restricted by the coupling of these atoms to subsurface layers. For example, the Si−O−Si bond angle formed when an O atom forms "bridge" bonds to two Si atoms on the Si(111) surface is smaller than the optimum Si−O−Si bond angle (e.g., in disiloxane), because the optimum surface structure is a compromise between opening the Si−O−Si angle and weakening the bonding between the surface and subsurface Si atoms. A molecular model of a surface that is large enough to capture this surface−subsurface coupling would almost certainly be too large for it to be represented using ab initio quantum mechanical (QM) computational methods. However, QM methods are needed to accurately model bond making and breaking reactions (e.g., surface adsorption and desorption). In order to produce a system that is large enough to be a realistic surface model and yet still suitable for practical calculations, one must either use a good (large) surface model with a less accurate computational method, or use a poorer (small) surface model with an entirely ab initio computational method.

The small molecular clusters used in ab initio models of surface chemistry are more accurately called reactive site models (RSMs) than surface models, since they typically contain a single surface reactive site along with its adjacent subsurface atoms. While these clusters are small enough for very accurate (multiconfiguration) ab initio calculations, the connection between such a calculation and the corresponding reaction on a real surface is unclear. Some researchers attempt to reproduce surface−subsurface coupling in these RSMs by fixing the positions of the subsurface atoms; however, this approach is restrictive. One desires instead a realistic, low computational cost method to reproduce subsurface coupling for ab initio calculations of RSMs.

Hybrid quantum mechanics/molecular mechanics (QM/MM) techniques are becoming increasing popular for modeling large molecular systems. In this approach, one assumes that a large molecular system can be partitioned into a small, chemically active site where a reaction will occur, and a larger, chemically inactive piece[2] (This assumption is sometimes complex, e.g., electronically delocalized systems such as graphite would be especially difficult to partition.) The chemically active site is modeled with QM, while the inactive part is modeled with MM. The mechanical influence of the inactive portion, provided by MM, constrains the geometry of the active site, and therefore has an indirect effect on its chemistry. The key to the success of a hybrid QM/MM technique is the manner in which the influence of the MM region is communicated to the QM region.

Weiner et al. developed a hybrid QM/MM method and applied it to the study of reactions of acetylene with silicon surfaces.[3] In their approach, the MM portion of the calculation determines the positions of the atoms at the boundary of the QM portion; this in turn restricts the displacement of surface Si atoms. Maseras and Morokuma have recently developed a hybrid QM/MM method called the integrated molecular orbital molecular mechanics (IMOMM) method. In IMOMM, the forces (energy gradients) exerted by the MM region onto the QM region are combined with the internal forces of the QM region, and this hybrid gradient is used to drive the optimization of the QM region.[4] IMOMM is a physically appealing way to couple MM and QM calculations, because the MM forces affect the entire RSM, not just the atoms on its boundary. However, as discussed below, the method used to link the QM and MM regions in the original IMOMM implementation will not work

[†] Present address: Lawrence Livermore National Laboratory, Livermore, CA 94550.

10.1021/jp982600e CCC: $18.00
Published on Web 04/10/1999

well for modeling surfaces. In addition, the usual internal coordinates (e.g., bond distances, bond angles, torsion angles) are inadequate for describing the highly coupled clusters used to simulate surfaces.

In the present paper, we present modifications to IMOMM that enable its application to modeling surfaces. We call this approach surface IMOMM, or SIMOMM. We compare our modified approach with Weiner's method for cluster models of the dimers on the Si(100) surface.

II. Design and Partitioning of a Surface Model

The overall procedure used to design a model system is essentially the same for any hybrid QM/MM approach. The differences between various QM/MM approaches arise in how the QM and MM portions of the model are linked, conceptually and mathematically. Additional problems arise for surface models, and this is the focus of the following discussion.

We begin by designing a large cluster model of the surface of interest. This cluster will have the structure of a bulk material, with one face of the cluster matching the surface of interest. The reactive site of interest should be at the center of the surface. We refer to this system as the bulk model (BM), because it is intended to model the mechanical behavior of bulk material. The majority of this cluster will be chemically inactive and thus is adequately modeled using MM. The size of this cluster is limited by the computational cost of the MM calculations, i.e., hundreds to thousands of atoms. Next, we carve out a chemically active subsection of the BM, which includes the surface reactive site plus its adjacent subsurface atoms. We refer to this chemically active subsection as the reactive site model (RSM). The RSM will be used in the QM part of the calculation, so its size is limited by the QM computational cost.

Creating the RSM by carving it out of the BM means that the RSM atoms adjacent to the cuts will possess unpaired electrons (dangling bonds). In a real material, the surface is usually reactive because the surface atoms are undercoordinated, while all the subsurface atoms are fully coordinated. The dangling bonds on the subsurface atoms in the RSM must be terminated; otherwise, the chemical behavior of the RSM will be dramatically different from a real surface. The dangling bonds of the RSM are typically saturated with H atoms to correct this problem, though one should be aware that H atom termination will not give an identical match of bonding in the bulk material.[5] The H atoms terminating the RSM do not exist in the BM. The treatment of these atoms in the transitions between the QM and MM stages is a key element of hybrid QM/MM methods.

IIA. Original IMOMM Method. The different regions in the IMOMM approach (note: ref 4 uses the term "set" instead of" region") are defined as follows:

Region 1 contains lattice atoms common to both the RSM and BM. These atoms are present in both the QM and MM portions of the calculation. Region 1 atom positions are allowed to move under the influence of a combined QM/MM gradient in the QM portion of the calculation, but their positions are fixed in the MM portion of the calculation.

Region 2 contains the H atoms used to terminate the dangling bonds created when the reactive site is cut out of the BM. *Region 2 atoms are present in only the QM calculation*, and their positions remain fixed.

Region 3 contains lattice atoms (*present only in the BM*) that are bonded to the Region 1 atoms. Region 3 atoms are present only in the MM calculation, and their positions remain fixed.

Region 4 is composed of lattice atoms in the BM not bonded to Region 1 atoms. *Region 4 atoms are present only in the MM calculation*, and they are allowed to move under the influence of only a MM gradient.

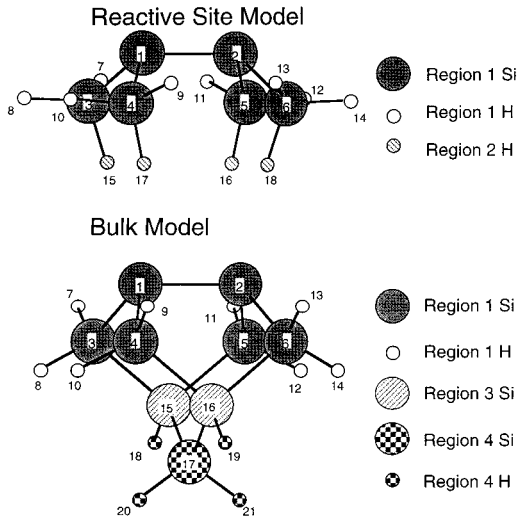

Figure 1. IMOMM partitioning scheme.

Figure 1 illustrates a specific example of a QM/MM system, Si_6H_{12}/Si_9H_{12}, using the IMOMM partitioning scheme. In this example, Si_6H_{12} is the RSM, and Si_9H_{12} is the BM. Atoms 1−14, Region 1, are the same in both the RSM and BM. H atoms 15−18 in the RSM are the Region 2 (link) atoms. In the BM, the Region 2 H atoms are replaced by Region 3 Si atoms 15−16. Atoms 17−21 of the BM comprise Region 4 and are not bonded to any Region 1 atoms.

This Si_6H_{12}/Si_9H_{12} QM/MM system is unusual because the number of Region 4 atoms is smaller than the number of Region 1 atoms. Since the computational cost of a MM calculation is so much lower than a QM calculation, an actual QM/MM system would typically have many more Region 4 than Region 1 atoms. However, the IMOMM partitioning scheme can be more clearly described on a simple system such as that in Figure 1.

The coupling between the QM and MM portions of the calculation (the chemically active and inactive regions) is determined by defining the relationship between Region 2 and Region 3 atoms. In IMOMM, this relationship is defined as follows. First, one defines the Region 1−Region 3 bond lengths and directions based on lattice parameters. Once specified, these R1−R3 bond lengths and directions remain fixed. The R1−R2 bond *directions* are also fixed at the R1−R3 values, but the R1−R2 bond *distances* are fixed at different, user-selected values. For example, for a silicon cluster, Region 1 would be Si atoms, Region 2 H atoms, and Region 3 Si atoms. The R1−R3 bond distance would be fixed at 2.35 Å, and the R3 positions chosen so that the R1Si−R1Si−R3Si angles and the R1Si−R1Si−R1Si−R3Si torsions are at silicon lattice values. The R1Si−R2H bond distances would be fixed at 1.48 Å, pointing along the R1Si−R3Si bond directions, so all R1Si−R1Si−R2H angles and R1Si−R1Si−R2H torsions are also at silicon lattice values.

IIB. Weiner Method. The IMOMM partitioning scheme can also be used to describe Weiner's QM/MM computational approach; however, atoms in Regions 2 and 3 are treated differently. In Weiner's method, the positions of the Region 3 atoms are determined by the MM optimization stage of the calculation, not predetermined by the user. The R1−R2 bond distances are set by the user, *but the R1−R2 bond directions are set to the R1−R3 values*. These fixed R1−R2 bond directions at the edge of the RSM will affect the bonding in

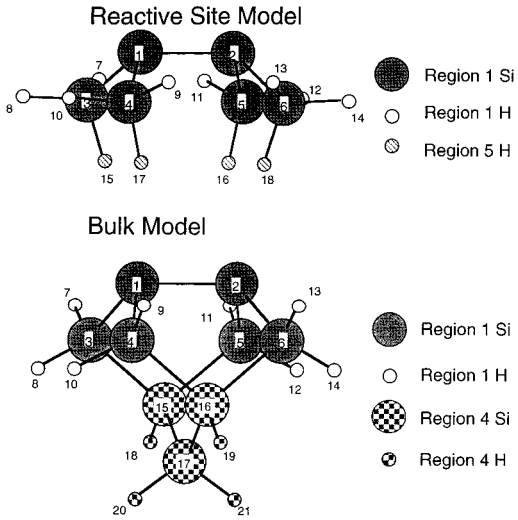

Figure 2. SIMOMM partitioning scheme.

the interior of the RSM, so in Weiner's method the influence of the BM on the RSM is transmitted through atom positions, while in IMOMM this influence is transmitted though forces.

IIC. Surface IMOMM. In addition to its conceptual simplicity, the R2−R3 method of linking the QM and MM portions of the model has the added benefit of reducing the mathematical complexity of IMOMM. (This will be discussed in section III.) However, this linking scheme causes some problems when used for surface models. In IMOMM, the positions of Regions 2 and 3 atoms are defined by the user and are not allowed to vary during the course of the calculation. For surface models, the high degree of connectivity in a lattice means there will be a large number of links between the RSM and BM, which results in the imposition of a large number of user-defined constraints. With so much of the model defined by the user, it is likely the user's choices will predetermine the answer. In addition, a one-to-one correspondence between R2 and R3 atoms is tacitly assumed in this linking scheme. For surface models, this will not always be true. As shown in Figure 1**,** both R2 atoms 15 and 16 (17 and 18) are related to R3 atom 15 (16). Defining the correct relative positions of all three atoms will be difficult and may also overly constrain the calculation. To ensure a one-to-one correspondence between R2 and R3 for this case, one would have to increase the size of the RSM, greatly increasing overall computational cost by increasing the size of the QM stage of the calculation.

The limitation of the R2−R3 linking scheme can be overcome by introducing a new set of atoms, which we call Region 5. In this scheme, we have the following:

Region 1 is defined as before.

Region 5 contains H atoms used to terminate the dangling bonds created when the reactive site is cut out of the BM. Region 5 atoms are present in only the QM calculation, *but their positions are allowed to move in response to only the QM gradient*.

Region 4 is composed of lattice atoms in the BM *including those that are bonded to Region 1*. Region 4 atoms are present only in the MM calculation, and they are allowed to move under the influence of only a MM gradient.

This new partitioning scheme is illustrated in Figure 2.

In the QM stage of an IMOMM calculation, Region 1 atom positions are free to move, e.g., in response to a reaction. Region 2 atoms also move, because they are bonded to Region 1 atoms, but the Region 2 positions relative to the Region 1 atoms remain fixed at user selected values. Similarly, in the MM stage of an IMOMM calculation, the relative positions of the BM atoms bonded to Region 1 atoms, those in Region 3, remain fixed at user selected values. Since the new partitioning eliminates both Region 2 and Region 3, *the user-defined constraints on the positions of the MM atoms bonded to Region 1 are also eliminated*. Now, when the Region 1 positions change during the QM stage of the calculation, the positions of the Region 4 atoms that are bonded to Region 1 are determined by the MM gradient minimization, *not the user*. We refer to the use of IMOMM with this alternative partitioning scheme as surface IMOMM (SIMOMM), since we anticipate that this partitioning scheme will be needed in QM/MM models of surfaces.

TABLE 1: Constraints Imposed on Atoms in the Three QM/MM Techniques Described

	IMOMM	SIMOMM	Weiner
R1 QM	optimized	optimized	optimized
R1 MM	fixed	fixed	fixed
R2 stretch	fixed	n/a	fixed
R2 bend	optimized	n/a	fixed
R2 torsion	optimized	n/a	fixed
R3 positions	fixed	n/a	optimized
R4 positions	optimized	optimized	optimized
R5 positions	n/a	either	either

Table 1 summarizes the treatment of atoms in the different regions in the hybrid clusters in IMOMM, SIMOMM, and Weiner's method. Of the three methods, SIMOMM has the smallest number of fixed variables, and so is least influenced by user choices. This also means that SIMOMM is most susceptible to failure resulting from a poorly designed model system.

III. Derivation of QM/MM Optimization Process

IIIA. Avoiding Double Counting. The MM stage of the QM/MM calculation is intended to provide external forces on the RSM. Region 1 atoms are present in both the QM and MM stages, so forces internal to Region 1 will be calculated in both stages. Thus, the MM stage must be modified to eliminate double counting of these same terms in the QM stage. Because MM interactions are described with interatomic potentials, the internal Region 1 terms can be readily identified and zeroed out. These modified MM equations are used in the formal derivation of the IMOMM optimization procedure. Reference 4 defines the following set of rules for modifying the MM energy and gradient calculations to eliminate this double counting:

1. Interactions involving atoms of Region 1 exclusively are neglected in the MM calculation, as Region 1 interactions are already accounted for in the QM stage.

2. Region 1−Region 3 interactions are neglected in the MM code, with the assumption that Region 1−Region 3 interactions are properly reproduced by Region 1−Region 2 interactions in the QM code.

3. "Nonbonded" (e.g., van der Waals) interactions *between* atoms of Region 3 are retained in the MM code. These terms are sensitive to the nature of the atom and are not adequately represented by the interactions between the Region 2 atoms (typically H atoms) in the ab initio calculation.

Any interaction involving one atom of Region 4 is retained

These rules governing the treatment of MM interactions for Regions 1 and 4 are also used in SIMOMM; however, the rules for Regions 2 and 3 do not apply because these regions do not exist in SIMOMM. The other difference in SIMOMM is that R1−R5 interactions are modeled in the QM code, but because

the R5 atom positions are allowed to optimize, the effect of R1−R5 interactions is assumed to be small.

The interpretation of the MM energy in a QM/MM calculation deserves some discussion. In a QM calculation, energies are defined with respect to *separated nuclei and electrons*. In MM calculations, energies are defined with respect to *separated atoms*. The sum of the QM and MM energies in a QM/MM calculation is meaningful only for comparisons with other QM/MM calculations on the same RSM/BM system. For example, the energy of reaction in a QM/MM calculation would be defined as

$$\Delta E(\text{reaction}) = \{E_{QM}(\text{products}) - E_{QM}(\text{reactants})\} + \{E_{MM}(\text{products}) - E_{MM}(\text{reactants})\} \quad (1)$$

Despite the fact that the QM and MM energies have different scales, their separate differences have the same chemical scale. Derivatives of the QM and MM energies with respect to position are on the same scale, so there is no ambiguity in the interpretation of the QM/MM gradient.

IIIB. IMOMM Gradient Derivation. Optimization of molecular geometry is essentially the minimization of the molecular gradient, so the formation of the hybrid QM/MM gradient is central to IMOMM. The following derivation of the energy and gradient equations for IMOMM is taken from ref 4, but is reproduced here to highlight the differences obtained by the use of Region 5 termination. (The terms in the MM stage that duplicate terms in the QM stage have already been zeroed out in the following derivation.)

In IMOMM, the atomic positions of the Region 3 atoms are taken to depend on Region 1 and Region 2,

$$\vec{R}_3 = \vec{R}_3(\vec{R}_1,\vec{R}_2) \quad (2)$$

Using eq 2, the total energy of the system, the sum of the QM and MM cluster energies, can be written as

$$E_{QM} = E_{QM}(\vec{R}_1,\vec{R}_2) \quad (3)$$

$$E_{MM} = E_{MM}(\vec{R}_1,\vec{R}_3(\vec{R}_1,\vec{R}_2),\vec{R}_4) = E_{MM}(\vec{R}_1,\vec{R}_2,\vec{R}_4) \quad (4)$$

$$E_T = E_{QM} + E_{MM} = E_T(\vec{R}_1,\vec{R}_2,\vec{R}_4) \quad (5)$$

Applying the chain rule to the calculation of the gradients

$$\frac{\partial E_T}{\partial \vec{R}_1} = \frac{\partial E_{QM}}{\partial \vec{R}_1} + \frac{\partial E_{MM}}{\partial \vec{R}_1} + \sum_{\vec{R}_3} \frac{\partial E_{MM}}{\partial \vec{R}_3}\frac{\partial \vec{R}_3}{\partial \vec{R}_1} \quad (6)$$

$$\frac{\partial E_T}{\partial \vec{R}_2} = \frac{\partial E_{QM}}{\partial \vec{R}_2} + \frac{\partial E_{MM}}{\partial \vec{R}_2} + \sum_{\vec{R}_3} \frac{\partial E_{MM}}{\partial \vec{R}_3}\frac{\partial \vec{R}_3}{\partial \vec{R}_2} \quad (7)$$

$$\frac{dE_T}{d\vec{R}_4} = \frac{\partial E_{MM}}{d\vec{R}_3} \quad (8)$$

In IMOMM, the bond separations $\vec{r}_{12}$ and $\vec{r}_{13}$ are frozen at some reasonable user selected value. In addition, the bond and dihedral angles between $\vec{R}_1,\vec{R}_2$, and $\vec{R}_1,\vec{R}_3$ are constrained to be the same. This choice of linking the QM and MM parts of the problem removes the dependence of $\vec{R}_3$ on $\vec{R}_1$ so

$$d\vec{R}_3/d\vec{R}_1 = 0 \quad (9)$$

With the bond distances frozen, and the angles kept the same,

$$\frac{d\vec{R}_3}{d\vec{R}_2} = \vec{I}, \quad \frac{\partial E_{MM}}{\partial \vec{R}_3} = \frac{\partial E_{MM}}{\partial \vec{R}_2} \quad (10)$$

where $\vec{I}$ is the identity matrix. Using eqs 9 and 10, eqs 6 and 7 become

$$\frac{dE_T}{d\vec{R}_1} = \frac{\partial E_{QM}}{d\vec{R}_1} + \frac{\partial E_{MM}}{d\vec{R}_1} \quad (11)$$

$$\frac{dE_T}{d\vec{R}_2} = \frac{\partial E_{QM}}{d\vec{R}_2} + \frac{\partial E_{MM}}{d\vec{R}_2} \quad (12)$$

Equations 2−12 define the formal optimization problem for IMOMM. As the Region 4 atom positions are allowed to freely optimize in the MM portion of IMOMM, eq 8 should go to zero (ideally) upon optimization, though in practice convergence is satisfied when the gradient falls below some small value. Attaining a small "residual" intra-Region 4 gradient is actually quite important, because some of the intra-Region 4 gradient will project onto Region 1 (in the conversion of the MM gradient to internal coordinates). If the convergence of the intra-Region 4 gradient is set too high, feedback of this residual can cause the overall optimization to diverge.

It should be noted that eqs 11 and 12 are only valid for internal coordinates, and so the formation of the hybrid gradient must be performed using internal coordinates. *This requirement of using internal coordinates in the hybrid procedure imposes significant practical problems in applying this technique to cluster models of surfaces.* The problem of constructing "good" sets of internal coordinates for surface models is discussed in section IIID.

IIIC. SIMOMM Gradient Derivation. The use of Region 5 termination in SIMOMM simplifies the formal optimization problem because atoms in Regions 2 and 3 do not exist in this approach, so terms involving $\vec{R}_2$ and $\vec{R}_3$ never appear in the optimization problem. We have

$$\frac{dE_T}{d\vec{R}_1} = \frac{\partial E_{QM}}{d\vec{R}_1} + \frac{\partial E_{MM}}{d\vec{R}_1} \quad (13)$$

$$\frac{dE_T}{d\vec{R}_5} = \frac{\partial E_{QM}}{d\vec{R}_5} \quad (14)$$

$$\frac{dE_T}{d\vec{R}_4} = \frac{\partial E_{MM}}{d\vec{R}_4} \quad (15)$$

Note that the elimination of Regions 2 and 3 also eliminates the need to use internal coordinates, though the use of internal coordinates is preferred in determining reaction pathways.

IIID. Internal Coordinates for Reactive Site Models. Application of IMOMM requires the specification of a set of internal coordinates to add the QM and MM gradients. One need not run the QM optimization in internal coordinates, though the MM and QM gradients need to be transformed to internal coordinates before they are added in the original IMOMM procedure. However, transition state searches and general mapping of potential energy surfaces are often aided by freezing internal coordinates, so the use of internal coordinates is preferred. As is true for any system, the choice of a set of internal coordinates is driven by the requirement that the

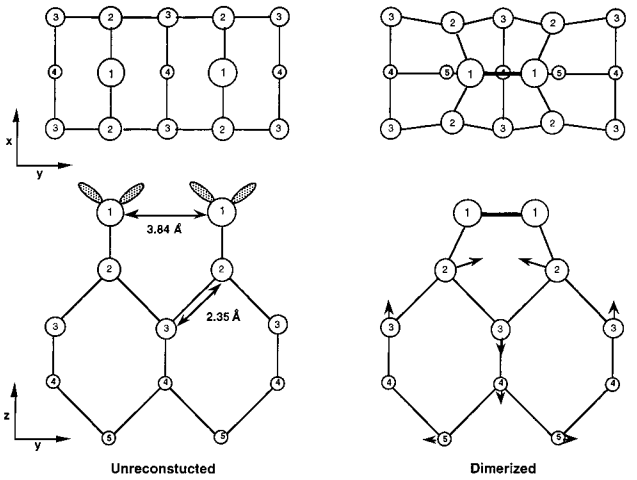

Figure 3. Formation of a dimer on the Si(001) surface. Surface atoms are labeled as layer 1. Decreasing size indicates increasing depth below the surface.

transformation matrix between Cartesian and internal coordinates is not near singular.

The use of internal coordinates for modeling surfaces with IMOMM is complicated by the fact that RSMs are pieces of crystal lattices, i.e., molecular cages. Specification of a good set of internal coordinates for a molecular cage is difficult because each atom is bonded to all its nearest neighbors, so that the total number of internal coordinates (stretches, angles, and torsions) that can be specified is much greater than the nonredundant internal degrees of freedom. Z-matrix internal coordinates almost always fail for such highly coupled systems. The natural internal coordinates developed by Pulay et al.[6] have been demonstrated to be very efficient internal coordinates for geometry optimizations. Unfortunately, natural internals also have difficulties with molecular cages. Redundant natural internals perform better on highly coupled systems; however, they can only be used with a redundant space optimization algorithm.[7] Baker et al. have recently described a set of symmetry coordinates, delocalized coordinates (DLCs), that are guaranteed to be orthogonal and nonredundant.[8] We have found that these DLCs perform very effectively for optimizations of cage molecules. As an added advantage, the algorithm for automatic specification of DLCs is rather simple, and because they are nonredundant, DLCs are easily used in conventional optimization schemes.

IIIE. Comparison of Methods. SIMOMM and Weiner's method were implemented using MM3[9] and GAMESS,[10] and compared in modeling the Si(001) 2 × 1 dimerized surface. (Other reconstructions of the Si(001) surface are possible; however, in this paper we limit the discussion to this specific reconstruction.) We selected the Si(001) dimerized surface for comparison of these methods because silicon surfaces have been extensively studied due to their importance in semiconductor fabrication. The formation of these dimer bonds illustrates the interplay between surface and subsurface atoms in a "surface" reaction.

Conceptually, a silicon (001) surface is created by cleaving a silicon lattice in a plane perpendicular to the (001) lattice direction. Initially, this cleavage leaves each Si atom at the surface with two unpaired electrons (dangling bonds). The orientation of the dangling bonds, illustrated in Figure 3, coupled with thermal motion of the lattice, favors formation of bonds between nearest neighbor Si atoms. There is singlet coupling between the remaining dangling bonds on the two atoms in the dimer, so the dimer bonds are singlet diradicals. The length of the dimer bonds, 2.25 Å, thus is smaller than the Si−Si lattice separation (single bond) of 2.35 Å, yet larger than the gas phase Si singlet diradical bond length of 2.16 Å calculated for Si_6H_{12}. During dimer bond formation, the nearest-neighbor surface atoms undergo large displacements from their initial lattice separations of 3.84 Å, dragging subsurface atoms along with them, and so the positions of the subsurface atoms are significantly displaced from their original lattice positions. However, the force (gradient) driving the formation of the dimer bond on the surface must compete with the forces holding the subsurface atoms near their lattice positions, thus the optimum length of the surface dimer is longer than the gas-phase value.

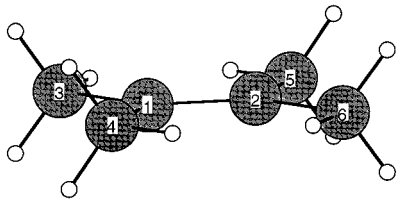

Figure 4. Si_6H_{12} GVB-PP(1) optimized geometry.

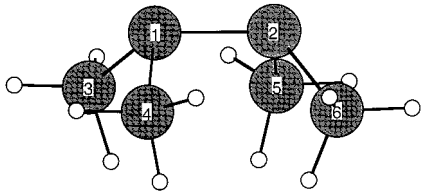

Figure 5. Si_6H_{12} SIMOMM optimized geometry.

For the hybrid QM/MM comparisons, we use Si_6H_{12} as the RSM for a single dimer. Since Si_6H_{12} includes the two atoms in the dimer and their nearest neighbors, it is the smallest reasonable model for a Si surface dimer, because the dimer atoms are bonded only to other Si atoms, as is true for a dimer on a real silicon surface. For the initial comparison, we use Si_9H_{12} (shown in Figure 1) as a model for bulk silicon. Si_9H_{12} is a very small cluster model of bulk silicon; however, because of its size we can readily compare full quantum optimizations of Si_9H_{12} with hybrid QM/MM optimizations of Si_6H_{12}. In the QM stage of the calculation, we model the Si dimer at the GVB-PP(1) level of theory, the simplest correct model for a singlet diradical, using the HW ECP basis set.[11] An ECP basis set was used for consistency with previous cluster models of a Si surface dimer, and because the primary concern here is comparisons of SIMOMM with Weiner's method, not in obtaining the most accurate results.

Figure 4 shows the GVB-PP(1) optimized geometry of Si_6H_{12}. Without the influence of MM forces from Si_9H_{12}, the silicons are all in the same plane. Figure 5 shows the SIMOMM (GVB-PP(1)/MM3) optimized geometry of Si_6H_{12}, incorporating forces from Si_9H_{12}. There is a huge qualitative difference between these two structures, illustrating the importance of including bulk mechanical effects in modeling surface reactions.

Table 2 presents a comparison of the SIMOMM and Weiner methods for the QM/MM optimization of the RSM Si_6H_{12} embedded in the BM Si_9H_{12}. (Region 5 termination was used for Weiner's method.) Also listed in this table are the GVB-PP(1) optimized geometry of Si_6H_{12}, Si_9H_{12}, and the MM3 optimized geometry of Si_9H_{12}. Overall, the differences between SIMOMM and Weiner's method for this case are small, the most noticeable observed in the torsion angles. The SIMOMM torsions agree better with the GVB-PP(1) optimized result for Si_9H_{12}. The MM3-optimized value for the silicon dimer bond

TABLE 2: Comparison of QM/MM Optimizations of Si_6H_{12} Embedded Cluster[a]

RSM (QM) / BM (MM)	Weiner Si_6H_{12} / Si_9H_{12}	SIMMOM Si_6H_{12} / Si_9H_{12}	GVB-PP(1) Si_6H_{12} / none	GVB-PP(1) Si_9H_{12} / none	MM none / Si_9H_{12}
dist (Å)					
2−1	2.278	2.261	2.159	2.249	2.376
3−1	2.333	2.338	2.332	2.329	2.352
4−1	2.333	2.338	2.332	2.329	2.352
5−2	2.345	2.338	2.332	2.329	2.352
6−2	2.345	2.338	2.332	2.329	2.352
angle (deg)					
3−1−2	109.850	108.507	121.672	106.491	103.906
4−1−2	109.867	108.526	121.672	106.491	103.906
5−2−1	109.859	108.513	121.672	106.491	103.906
6−2−1	109.839	108.494	121.672	106.491	103.906
3−1−4	112.007	109.287	116.655	111.006	108.461
5−2−6	112.034	109.287	116.654	111.006	108.461
torsion (deg)					
3−1−2−5	0.000	−0.003	0.000	0.000	0.000
4−1−2−3	123.645	118.654	0.000	118.254	113.414
6−2−1−5	−123.666	−118.665	0.000	−118.254	−113.414

[a] QM calculations are GVB-PP(1), HW ECP basis set.

TABLE 3: Comparison of Embedding Schemes on $Si_6H_{12}/Si_{38}H_{36}$ Hybrid Cluster[a]

RSM (QM) / BM (MM)	Weiner Si_6H_{12} / $Si_{38}H_{36}$	SIMMOM Si_6H_{12} / $Si_{38}H_{36}$	GVB-PP(1) Si_6H_{12} / none	GVB-PP(1) $Si_{38}H_{36}$ / none	MM none / $Si_{38}H_{36}$
dist (Å)					
2−1	2.277	2.254	2.159	2.281	2.370
3−1	2.332	2.342	2.332	2.349	2.350
4−1	2.333	2.342	2.332	2.349	2.350
5−2	2.346	2.342	2.332	2.349	2.350
6−2	2.346	2.342	2.332	2.349	2.350
angle (deg)					
3−1−2	109.850	108.035	121.672	105.550	104.252
4−1−2	109.866	108.039	121.672	105.550	104.252
5−2−1	109.860	108.038	121.672	105.550	104.252
6−2−1	109.84	108.034	121.672	105.550	104.252
3−1−4	112.006	115.721	116.655	115.879	112.858
5−2−6	112.034	115.699	116.654	115.879	112.858
torsion (deg)					
3−1−2−5	0.000	−0.005	0.000	0.000	0.000
4−1−2−3	123.645	125.878	0.000	123.213	118.557
6−2−1−5	−123.660	−125.842	0.000	−123.218	−118.557

[a] Ab initio calculations are GVB-PP(1), HW ECP basis set.

(2−1) of 2.376 Å is interesting, because it highlights a significant limitation of MM methods. The MM3 force field is only parametrized for sp^3 hybridization and therefore treats undercoordinated Si atoms in the same manner as fully coordinated Si. MM3 does not exactly reproduce the forces in the QM calculations, so the SIMOMM optimized results are different from the GVB-PP(1) optimization of Si_9H_{12}, but the differences are similar in magnitude to those reported for IMOMM (refs 4 and 12). Weiner's method requires 37 CPU minutes on a Sun Sparc 20 workstation compared with 107 min for SIMOMM. This time difference results from the fact that many more internal coordinates in the RSM are frozen in Weiner's method.

Since the ability of Si_9H_{12} to represent bulk silicon is questionable, the next step is to increase the size of the BM to evaluate the effect on the geometry of the embedded RSM. Figure 6 shows $Si_{38}H_{36}$, with the RSM atoms highlighted. Compared with Si9H12, $Si_{38}H_{36}$ contains subsurface Si atoms in addition to those directly under the surface dimer, so this larger BM should impose lateral as well as vertical steric constraints on the RSM. Table 3 lists a comparison of the SIMOMM and Weiner methods, together with a GVB-PP(1) optimization (using C_{2v} symmetry) for the entire BM. As in the previous case, we see small differences between the two hybrid QM/MM methods and the QM optimization of the full

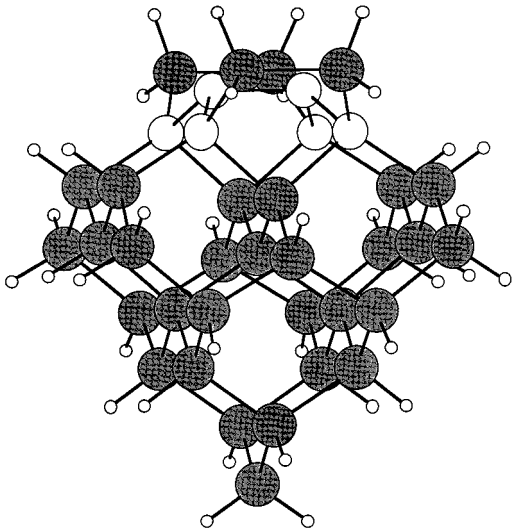

Figure 6. $Si_6H_{12}/Si_{38}H_{36}$ hybrid cluster. The six Region 1 Si atoms are highlighted.

TABLE 4: Timing Comparison for SIMOMM and Full QM Optimizations

SIMOMM GVB-PP(1)/MM3 Sparc 20, 1 cpu		GVB-PP(1) C_{2v} symmetry origin 2000, 16 cpus	
Si_6H_{12}/Si_9H_{12}	71 min	Si_9H_{12}	6 min
$Si_6H_{12}/Si_{38}H_{36}$	101 min	$Si_{38}H_{36}$	842 min

BM. Interestingly, these results for the dimer also show small differences from the cases which used Si_9H_{12} as the BM. These results suggest that Si_9H_{12} captures the most significant steric effects of bulk silicon on a single surface dimer.

IV. Conclusions

In this paper, we have presented an extension of the successful IMOMM method of Maseras and Morokuma that facilitates the treatment of surface chemistry using an embedded cluster model, SIMOMM. We have shown that including bulk mechanical effects can have a large effect on the optimized geometry of a reactive site model (RSM). For the cases discussed in this paper, the geometry of the RSM was not sensitive to the method with which the QM and MM regions were merged, though we do not expect this to be true in general. While a hybrid QM/MM model will not be as accurate as a full QM model, enormous time savings can be realized. Table 4 shows a comparison of the computational cost of SIMOMM and full QM calculations. For the larger system, SIMOMM is approximately 100 times faster. This time reduction is especially important for surface chemistry, for which one frequently needs to investigate a number of possible adsorption sites for a given adsorbate. Using SIMOMM, we have recently evaluated a number of O atom adsorption sites on Si- and C-terminated SiC(111) surfaces, requiring over a hundred separate calculations, in a matter of months.[13] A full QM treatment for *one* of these calculations would have taken over a year.

Acknowledgment. The authors are grateful to Dr. Feliu Maseras and Dr. Mike Schmidt for their helpful discussions. MSG is grateful for the support of the Air Force Office of Scientific Research. This work was supported by a grant of computer time by the DoD CHSSI program.

References and Notes

(1) Felici, R.; Robinson, I. K.; Ottaviani, C.; Imperatori, P.; Eng, P.; Perfetti, P. *Surf. Sci*. **1997**, *55*, 375.

(2) Field, M.; Gao, J. *Int. J. Comput. Chem*. **1996**, *60*, 1093.

(3) Weiner, B.; Carmer, C. S.; Frenklach, M. *Phys. Rev. B* **1991**, *43*, 1678. Carmer, C. S.; Weiner, B.; Frenklench, M. *J. Chem. Phys.* **1993**, *99*, 1356.

(4) Maseras, F.; Morokuma, K. *J. Comput. Chem.* **1995**, *16*, 1170.

(5) Sauer, J. *Chem. Rev.* **1989**, *89*, 199.

(6) Pulay, P.; Fogarasi, G.; Pang, F.; Boggs, J. E. *J. Am. Chem. Soc.* **1979**, *101*, 2550. Forages, G.; Shoo, X.; Taylor, P. W.; Pulay, P. *J. Am. Chem. Soc.* **1992**, *114*, 8191.

(7) Pulay, P.; Fogarasi, G. *J. Chem. Phys.* **1992**, *96*, 2856.

(8) Baker, J.; Kessi, A.; Delley, B. *J. Chem. Phys.* **1996**, *105*, 192.

(9) Allinger, N. L.; Yuh, Y. H.; Lii, J.-H. *J. Am. Chem. Soc.* **1989**, *111*, 8551.

(10) Schmidt, M. W.; Baldridge, K. K.; Boatz, J. A.; Elbert, S. T.; Gordon, M. S.; Jensen, J. H.; Koseki, S.; Matsunaga, N.; Nguyen, K. A.; Su, S. J.; Windus, T. L.; Dupuis, M.; Montgomery, J. A. *J. Comput. Chem.* **1993**, *14*, 1347.

(11) Hay, P. J.; Wadt, W. R. *J. Chem. Phys*. **1985**, *82*, 270.

(12) Matsubara, T.; Maseras, F.; Koga, N.; Morokuma, K. *J. Am. Chem. Soc*. **1996**, *100*, 2573.

(13) Manuscript in preparation.